

## A Chlorinated Polymer Promoted Analogue Co-Donors for Efficient Ternary All-Polymer Solar Cells

Hui Chen<sup>1</sup>, Yikun Guo<sup>2</sup>, Pengjie Chao<sup>1</sup>, Longzhu Liu<sup>1</sup>, Wei Chen<sup>3,4</sup>, Dahui Zhao<sup>2\*</sup> & Feng He<sup>1\*</sup>

<sup>1</sup>Department of Chemistry and Shenzhen Grubbs Institute, Southern University of Science and Technology, Shenzhen 518055, China

<sup>2</sup>Beijing National Laboratory for Molecular Sciences, Center for Soft Matter Science and Engineering, Key Lab of Polymer Chemistry & Physics of the Ministry of Education, College of Chemistry, Peking University, Beijing 100871, China

<sup>3</sup>Materials Science Division, Argonne National Laboratory, 9700 Cass Avenue, Lemont, Illinois, 60439, United States.

<sup>4</sup>Institute for Molecular Engineering, The University of Chicago, 5640 South Ellis Avenue, Chicago, Illinois, 60637, United States

Received \*\*\*; accepted \*\*\*; published online \*\*\*

The efficient ternary all-polymer solar cells (PSCs) are designed and fabricated, using a polymer acceptor of NDP-V-C7 and analogue co-donors containing a chlorinated polymer PBCIT and classical PTB7-Th. PBCIT and PTB7-Th possess very similar chemical structure and matched energy levels to form the cascade of the co-donors. Meanwhile, benefiting from those analogous polymer structures, there is little influence of the morphology in blend film compared to their pristine polymer films. The binary PBCIT:NDP-V-C7 devices exhibit a high open-circuit voltage ( $V_{oc}$ ) due to the deep HOMO level of PBCIT. The  $V_{oc}$  of all-PSCs could be finely manipulated by adjusting the content of PBCIT in blend film. The ternary all-PSCs have the more balanced charge mobility and prolonged carrier lifetime compared to the binary devices. The PBCIT also help improve the miscibility of ternary blend and suppress crystallization in films, bringing about favorable morphology with appropriate orientation and surface roughness in blend film. With the optimal processing, the champion ternary all-PSCs obtain a high PCE of 9.03%, which is about 10% enhancement compared to that of binary device. The results indicate that the ternary approach using analogue co-donors is a practical method to enhance the performance of all-PSCs.

**All-polymer solar cells, chlorination, analogue co-donors, ternary blend, carriers transport**

**Citation:** Zhang TX, Familyname F, Familyname MF. Title: a concise and characteristic description of the involved research content with no more than 20 words. *Sci China Chem.* \*\*\*, doi: \*\*\*

### 1 Introduction

The solution-processed polymer solar cells with bulk-heterojunction (BHJ) have made great progress in the past decade.[1-10] they possess some appealing advantage including lightweight, low-cost, flexible and potential for large-scale area devices.[11-14] Through the advances of polymer design and device processing, the power conversion efficiency (PCE) of fullerene-based PSCs has been over 12%,[15] the

PCEs beyond 14% have obtained for PSCs based on non-fullerene small molecule acceptor.[16-21] Apart from the fullerene derivatives and non-fullerene small molecule acceptors, the polymeric acceptor is also an alternative candidate for PSCs.[22-24] The structural and optoelectronic properties of acceptor polymer can be designed and tuned like donor polymer, so the all-PSCs using donor and acceptor polymer provide some advantages for enhancement of PSC performance. The polymer donor and acceptor can have complementary range of absorption spectrum to increase photon harvesting. The entire film from polymer donor and acceptor, is potential to preferable morphology with interpenetrating

\*Corresponding authors (email: hef@sustc.edu.cn; dhzhao@pku.edu.cn)

network in BHJ active layer. The optimal morphology is benefit to exciton generation and charge carrier transport in blend film. Additionally, all-PSCs have several unique merits containing lower cost, better mechanical behavior, and superior stability of morphology compared to the PSCs using fullerenes and small molecule acceptors. [25-30]

Through the innovation of polymer acceptor design and evolutive device processing, the efficiencies of all-PSCs have been boomed in recent years, the recorded PCE was up to 10% reported by employing naphthalene-diiimide (NDI) derivative N2200 as polymer acceptor in Huang's group.[31] To date, NDI and perylene-diiimide (PDI) derivatives are the representative polymer acceptors due to their facile synthetic routes, adjustable levels of energy, and approving electron mobilities.[32-33] Although the binary all-PSCs have abundant progress, the narrow absorption range of blend active layer hinders the device performance. To further improve the PCE of all-PSCs, the ternary approach is a facile method to better sunlight absorption and charge carrier transfer.[34-35] Compared to tandem PSCs, the ternary PSCs maintain the simplified fabrication without complicated processing and preparation period. The ternary PSCs using two donors and an acceptor or a donor and two acceptors have been

extensively researched and obtained many encouraging advances. [36-39] Recently, we have designed and developed chlorinated family of polymer donors for both fullerene and non-fullerene PSCs.[40-42] The results demonstrated that chlorination can finely manipulate open-circuit voltage ( $V_{oc}$ ) in PSCs, attributing to the blueshift of absorb spectra and deep HOMO levels of chlorinated polymers. Thus, the chlorinated polymer donors have the potential to extend to the all-PSCs considered its spectra blueshift and better coverage from the whole sunlight spectrum with other active components.

In this study, we fabricated an efficient ternary all-PSCs by introducing a chlorinated polymer donor named PBCIT [41] as an additional donor into PTB7-Th and NDP-V-C7[32] blend films. The binary all-PSCs using PBCIT has a moderate PCE of 6.44%, but the  $V_{oc}$  value is rather high, up to 0.93 V. The PBCIT and PTB7-Th are belonging to well-known PTB family polymers with TT and BDT units, they have very similar structure, and could form a kind of intimate complex like "polymer alloy" in blend films because they are analogs and have good compatibility from the film morphology. [33] With the optimizing of PBCIT contents, the chlorinated ternary all-PSCs pushed the PCE to 9.03%. The enhanced

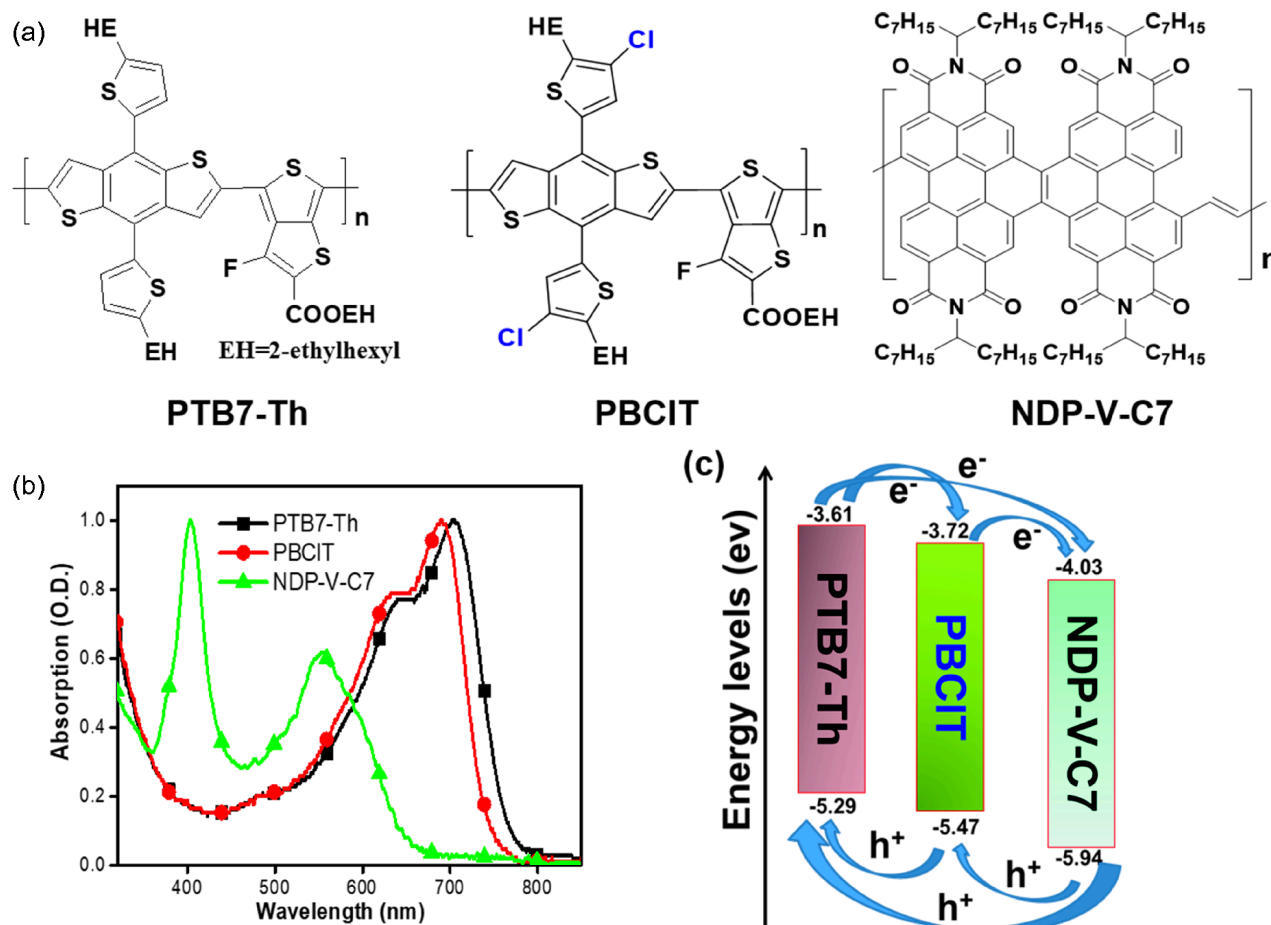


**Figure 1** (a) Chemical structures of PTB7-Th, PBCIT and NDP-V-C7; (b) Normalized UV-Vis absorptions of PTB7-Th, PBCIT and NDP-V-C7 films; (c) The molecular energy levels of PTB7-Th, PBCIT and NDP-V-C7.

performance ascribed increased  $V_{oc}$  and FF due to enhanced build-in potential and morphology via importing PBCIT. The results indicate that ternary approach, especially using polymer analogs with different absorption peaks as co-donors, is an effective measurement to boost the PCE of all-PSCs. It will give very similar polymer morphology packing in binary system with broad coverage of the sunlight resource.

## 2 Results and discussion

### 2.1 Chemical Structures, Optical and Electrical Properties

The Figure 1a depicts the chemical structures of PTB7-Th, PBCIT and NDP-V-C7, respectively. The polymer NDP-V-C7 as an efficient acceptor was reported before.[32] The PTB7-Th and PBCIT are the analogs in PTB family polymers with only two chlorine atoms difference in polymer conjugated side chains. The PBCIT shows slightly blue-shifted absorb spectra and rather deep HOMO level compared with PTB7-Th because of chlorination on the on side-chains of BDT unit as reported in previous study.[41] The molecular weight and molecular weight distribution of the polymers are summarized in Table S1. The Figure 1b shows the normalized UV-Vis absorptions and molecular energy levels of PTB7-Th, PBCIT and NDP-V-C7. Owing to the strong electrophilic effect of the two chlorine atoms, the LUMO and HOMO levels of PBCIT were obvious declined compared to PTB7-Th from Figure 1c. As discussed in this ternary system, the final LUMO and HOMO levels of PBCIT just fall in between those of PTB7-Th and NDP-V-C7. The stepped molecular energy levels of three polymers form a cascade charge transfer for electrons and holes in operation of ternary all-PSCs. The enough energy offsets among the two donors and a acceptor provide the sufficient driving force to dissociate the excitons.[39]

### 2.2 Photovoltaic Performance

To explore the device performance of ternary all-PSCs, we fabricated the inverted devices using a structure of ITO/ZnO/PTB7-Th:PBCIT:NDP-V-C7/MoO<sub>3</sub>/Ag. The current density-voltage ( $J$ - $V$ ) curves of the binary and champion ternary all-PSCs under 100 mW cm<sup>-2</sup> AM 1.5 G irradiation are presented in Figure 2a. The detail device parameters of ternary all-PSCs with different mass ratios of PTB7-Th and PBCIT are summarized in Table 1. The initial binary device based on PTB7-Th: NDP-V-C7 had a decent PCE of 8.27%,  $J_{sc}$  of 16.93 mA cm<sup>-2</sup> and FF of 65.48%, but the moderate  $V_{oc}$  of 0.75 V hindered the further efficiency of device. On the contrary, the PBCIT: NDP-V-C7 based binary all-PSCs showed a lower PCE of 6.44,  $J_{sc}$  of 12.91 mA cm<sup>-2</sup> and FF of 53.56%, while the  $V_{oc}$  was up to 0.93 V and a rather high value in the all-PSCs. The chlorinated PBCIT possessed a relatively deep HOMO, leading a higher  $V_{oc}$  in the device from the previous reports. The above results gave us a hint

which could unite the advantages of PTB7 and PBCIT to enhance the all-PSCs performance. By gradually increasing the content of PBCIT in ternary all-PSCs, the  $V_{oc}$  of relevant devices were monotonous improved and linearly fitted in Figure S1a. When the content of PBCIT was at 10% in donors, the  $J_{sc}$  and FF had some neglectable decline (Figure S1b-c), the PCE of device was slightly push to 8.46%. By continue adding the ratio of PBCIT was at 15%, the champion ternary all-PSCs were obtained, the PCE of device was 9.03% with the simultaneously increased  $V_{oc}$ ,  $J_{sc}$  and FF. To gradually raise the PBCIT content, the  $J_{sc}$  and FF was decreased obviously, leading to poor device performance (Figure S1d). The origin is that the PBCIT has a deeper HOMO level compared to PTB7-Th, and the homologous molecular structure facilitates to form intimate mixture as a new alloy donor.[43] The variation trend of  $J_{sc}$  and FF was diverse and like a parabola,

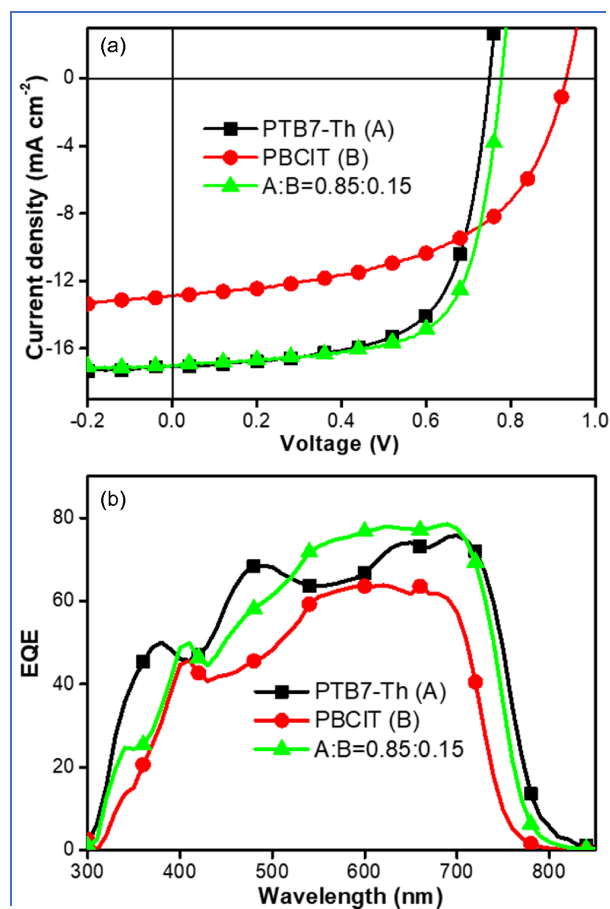


**Figure 2** (a)  $J$ - $V$  and EQE curves of binary and champion ternary all-PSCs.

the PBCIT content is the crucial factor to tune the device performance in ternary blend.

To better comprehend the reason of enhanced ternary all-PSCs, we conducted blend film absorption (Figure S2) and the external quantum efficiency (EQE) of binary and ternary device in Figure 2b. The ternary device with 15% PBCIT content was selected as investigative object due to the highest device performance with this ratio among the all proportion. Both the absorption of pure polymers and blending with

**Table 1** The performance parameters of ternary PSCs with various mass ratios of donors under 100 mW cm<sup>-2</sup> AM 1.5 G irradiation.

PTB7-Th: PBCIT	$V_{oc}$ [V]	$J_{sc}$ [mA cm <sup>-2</sup> ]	FF [%]	PCE <sup>a)</sup> [%]	PCE <sub>max</sub> [%]
1.00 : 0.00	0.75	16.73 ± 0.18	65.01 ± 0.48	8.15 ± 0.11	8.27
0.90 : 0.10	0.77	16.68 ± 0.23	64.68 ± 0.47	8.31 ± 0.13	8.46
0.85 : 0.15	0.78	16.77 ± 0.21	68.07 ± 0.39	8.97 ± 0.07	9.03
0.80 : 0.20	0.79	16.25 ± 0.19	65.12 ± 0.58	8.42 ± 0.10	8.53
0.70 : 0.30	0.80	15.01 ± 0.16	63.03 ± 0.41	7.49 ± 0.13	7.67
0.50 : 0.50	0.83	14.02 ± 0.13	59.27 ± 0.38	6.94 ± 0.07	7.01
0.25 : 0.75	0.88	13.45 ± 0.11	49.17 ± 0.42	5.80 ± 0.09	5.92
0.00 : 1.00	0.93	12.78 ± 0.08	53.21 ± 0.35	6.29 ± 0.10	6.44

<sup>a</sup>Average value ± standard deviation were calculated from 20 independent devices.

NDP-V-C7 films, the PTB7-Th with 15% PBCIT produced the somewhat blueshift of spectra on account of chlorine atom with some unique merits as previous reports. As well, compared with binary PTB7-Th: NDP-V-C7 device, the ternary device exhibited a little narrower response range from the EQE curves. The interesting result is that the  $J_{sc}$  of the ternary device was not decreased and slightly increased, attributing to the remarkable enhancement of photo-response from 500 to 750 nm. The integrated currents from EQE curves matches well with the extracted values from  $J$ - $V$  curves.

### 2.3 Investigation of Charge Dynamics

To understand the excitation dissociation state in all-PSCs, the photoluminescence (PL) spectra of donors and related blend films were determined in Figure 3(a). The donors films both had characteristic PL emission peaks.[44] When blended with NDP-V-C7, the PBCIT:NDP-V-C7 film also had a distinct peak at 800 nm, but the PTB7-Th:NDP-V-C7 and PTB7-Th:PBCIT:NDP-V-C7 films were almost completely quenched. Referring to the devices performance, the charge

separation of ternary device was neatly equal to binary device with PTB7-Th, surpassing the binary PBCIT based device. We tested the  $J_{sc}$  of devices under different light intensities ( $I$ ) to probe the recombination dynamics of carriers. The  $J_{sc}$  and  $I$  can be depicted[45] by a function of  $J_{sc} \propto I^\alpha$ , the  $\alpha$  is the slope at the double logarithmic coordinates plot. From the fitted curves in Figure 3(b), the  $\alpha$  values of binary PTB7-Th and PBCIT based devices were 0.95 and 0.91, respectively. As expected, the optimized ternary device had a highest  $\alpha$  value of 0.97, illustrating that the ternary blend would restrain the bimolecular recombination in devices.

Then, we determined the hole and electron mobility of devices[46] in Figure S3 and Table S2 as well. The hole mobility of devices based on PTB7-Th, PBCIT and mixed PTB7-Th:PBCIT were  $6.7 \times 10^{-4}$  cm<sup>2</sup> V<sup>-1</sup> S<sup>-1</sup>,  $1.5 \times 10^{-4}$  cm<sup>2</sup> V<sup>-1</sup> S<sup>-1</sup>, and  $3.7 \times 10^{-4}$  cm<sup>2</sup> V<sup>-1</sup> S<sup>-1</sup>, respectively. The corresponding electron mobility were  $2.1 \times 10^{-4}$  cm<sup>2</sup> V<sup>-1</sup> S<sup>-1</sup>,  $3.7 \times 10^{-5}$  cm<sup>2</sup> V<sup>-1</sup> S<sup>-1</sup>, and  $1.8 \times 10^{-4}$  cm<sup>2</sup> V<sup>-1</sup> S<sup>-1</sup>, respectively. Although the ternary device had no highest mobility among of the devices, the balanced ratio of hole and electron mobility

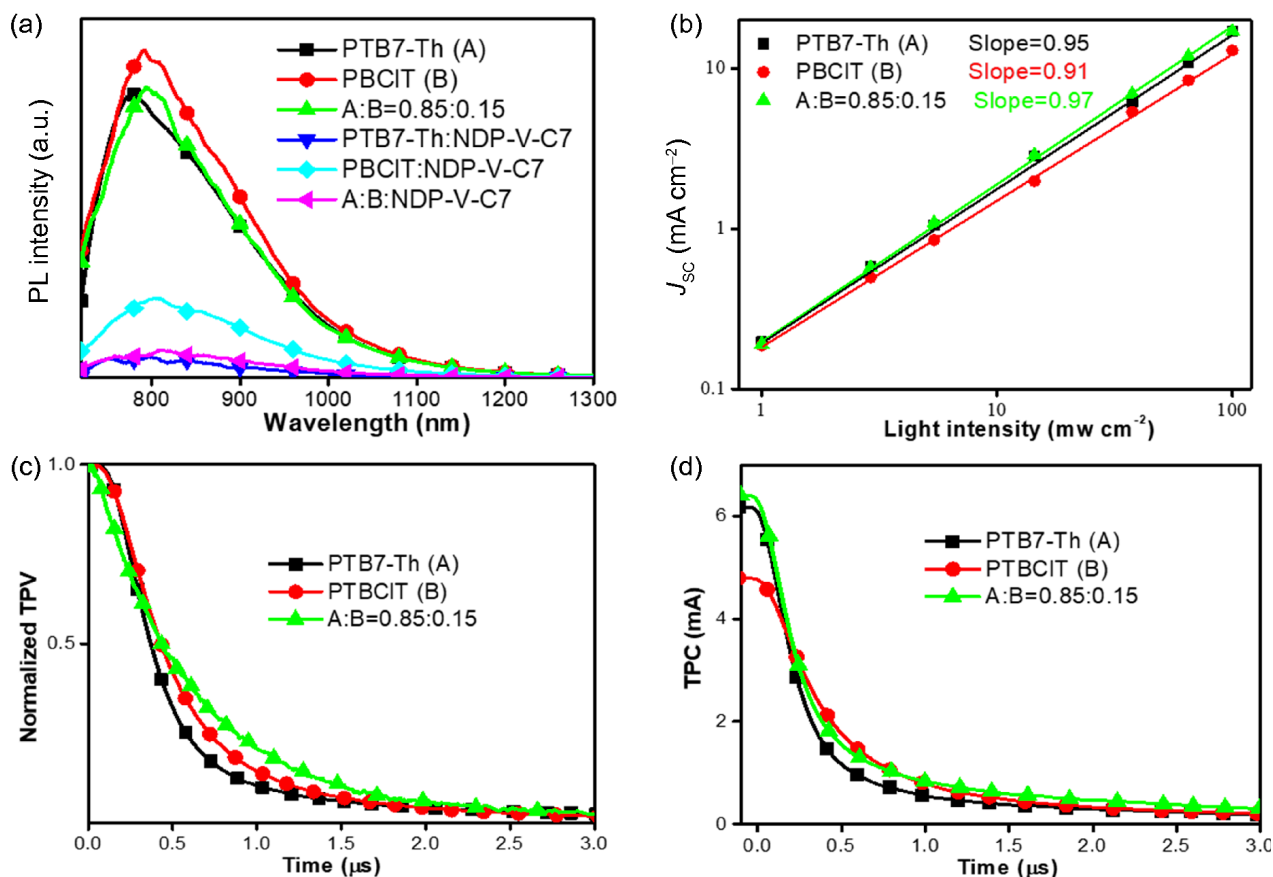


**Figure 3** (a) The PL spectra of neat polymer and blend films; Experimental  $J_{sc}$  versus light intensity (b), normalized TPV (c) and TPC (d) for binary and champion ternary devices, respectively.

is 2.1, being inferior to the 3.2 and 4.1 of binary devices. The balance of carriers transport is conducive to reducing the charge accumulation in devices, so that the ternary device obtains the good  $J_{sc}$  and FF. To further find out the carriers dynamics behavior in devices, the transient photovoltage (TPV) technology[47] was used to determine the carrier lifetime ( $\tau$ ) in device operation under open circuit. The Figure 5(c) is the normalized results, the extracted values of  $\tau$  from single exponential fitting were shown in Table S3. The  $\tau$  of devices based on PTB7-Th, PBCIT and mixed PTB7-Th:PBCIT were 0.40, 0.49 and 0.59  $\mu$ s, respectively. The prolonged carrier lifetime could enhance the charge transport and also supported the investigation of reduced bimolecular recombination. We utilized the transient photocurrent (TPC) measurement[48] to analyse the carriers extraction in device under short circuit. The determined sweeping out times ( $t_s$ ) of carriers were also present in Table S3. The  $t_s$  of PBCIT based device was 0.54  $\mu$ s, the overmoderated extraction hampered charge collection at electrode in device, which generated the lower  $J_{sc}$  and FF in related devices. The recombination and extraction of carriers were concurred and completed, the ratio of  $\tau$  and  $t_s$  could reflect integrated qualities of carriers.[48] The ternary device with high ratio of 1.97 from Table S3 indicated the prominent charge transport and

collection in the device, which is in agreement with the above  $J_{sc}$  and FF results.

## 2.4 Thermodynamics Analysis

The compatibility of acceptor and donor is a key factor for the domain distribution of blend film and related device performance. We took the differential scanning calorimetry (DSC) technique to research the thermodynamic properties of neat and blend films.[27] The neat NDP-V-C7 acceptor had two semi-crystalline regions: the region I around 185 °C and region II around 270 °C upon cooling stage from Figure 4 and Figure S4. But no observed thermal transition was appeared both in neat PTB7-Th and PBCIT polymer (Figure S5 and S6) The semi-crystalline region I was weakened and region II was almost vanished in PTB7-Th:NDP-V-C7 blend as plotted in Figure 4 and Figure S7, this phenomenon indicated the PTB7-Th could partly control the crystallization in blend with NDP-V-C7. Interestingly, the semi-crystalline region I and II were both not emerged in PBCIT:NDP-V-C7 blend from Figure 4 and Figure S8, the crystallization was almost entirely suppressed.[41] The PBCIT and NDP-V-C7 presented a favorable miscibility in their blend, which should benefit from the special intermolecular interactions of

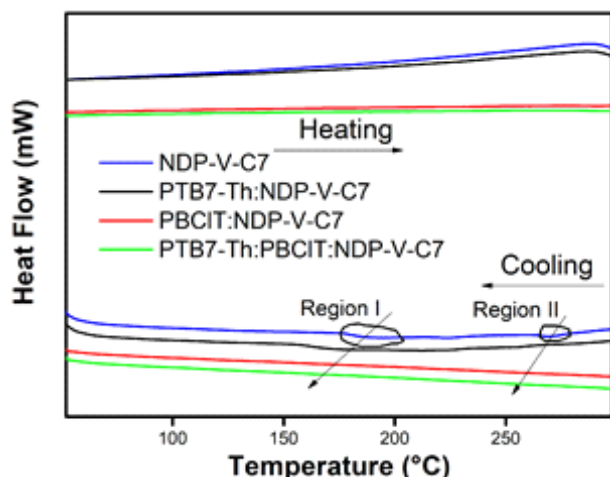


**Figure 4** DSC traces of NDP-V-C7 and their blend containing binary and ternary.

chlorine atoms with acceptor polymer. Thus, when the PBCIT as third component added in PTB7-Th:NDP-V-C7 blend, the crystallization could be further declined in new ternary blend films as shown in Figure 4, in which the two semi-crystalline regions in NDP-V-C7 had been found to totally vanish. This inference was also evidenced in DSC plot of ternary blend from Figure S9. The enhanced miscibility could optimize the morphology and improve device performance

via incorporating PBCIT into PTB7-Th:NDP-V-C7 blend film.

## 2.5 Morphology Study

To further explore the relationship between the morphology and device performance, we used the grazing incident wide-angle X-ray scattering (GIWAXS) to research the molecular packing and orientation in the binary and ternary blend films.[49] The blend films presented the similar diffraction patterns and line-cuts in out-of-plane (OOP) and in-plane (IP) from the Figure 5, which may come from the similar structure of PTB7-Th and PBCIT, both of them belongs to PTB family polymers. In the Figure 5(d), all the blend films have obvious  $\pi$ - $\pi$  stacking signal peaks at  $\sim 1.58 \text{ \AA}^{-1}$ , indicating distance of  $3.97 \text{ \AA}$ . But the full width at half-maximum (FWHM) of PBCIT is  $0.61 \text{ \AA}^{-1}$ , which is larger than  $0.50 \text{ \AA}^{-1}$  of PTB7-Th. The blend film with PTB7-Th has more favorable face-on orientation and crystalline content than the PBCIT blend film, the superior morphology features is benefit to helping excitons' dissociation and carriers' diffusion, according with the performance of corresponding devices. The morphology behavior of ternary blend film was similar to that of the binary film with PTB7-Th, this phenomenon implied that incorporating 15% PBCIT in donors barely changed the initial patterns of molecular packing and

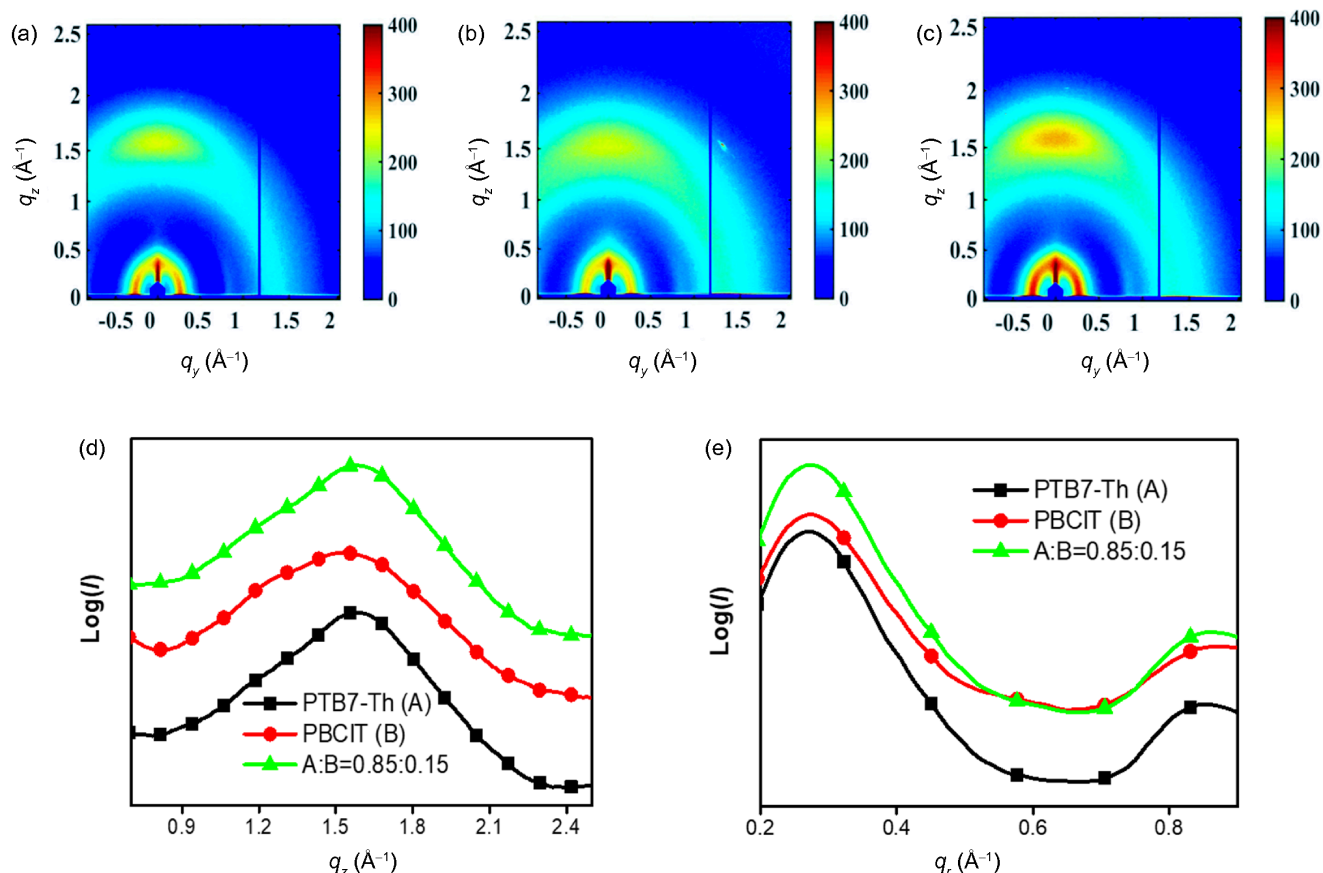


**Figure 5** GIWAXS patterns of PTB7-Th (a), PBCIT (b) and PTB7-Th:PBCIT (0.85:0.15) (c) films blending with NDP-V-C7; the related line-cuts in the out-of-plane (d) and in-plane (e).

orientation in the formed ternary blend film. The similar case was also observed in Figure 5(e). Thus, the  $J_{sc}$  and FF of optimal ternary device were not only declined compared to PTB7-Th based binary device, but also were a bit improved because of other virtues via introducing chlorinated polymer PBCIT.

We also used the transmission electron microscopy (TEM) and atomic force microscopy (AFM) to investigate the influence of PBCIT on phase separation and surface morphology of the blend films, the images were shown in Figure S10 and S11. The blend film with PTB7-Th:NDP-V-C7 exhibited flat and uniform feature, the PBCIT blend films had an apparent aggregation in their TEM images. To integrate the traits of binary blend film, the ternary blend film formed a desired phase separation profile from the TEM image. On the other hand, the PTB7-Th:NDP-V-C7 blend film had a smaller root-mean-square (RMS) roughness value of 0.78 nm from the AFM image, meanwhile the RMS value of blend film with PBCIT was 0.98 nm. The ternary blend film owned an appropriate RMS value of 0.86 nm between the those of PTB7-T and PBCIT films blending with NDP-V-C7. The acceptable coarse surface could provide the proper scale of phase separation promoting dissociation of excitons, the smooth surface also would form a favorable contact with interfacial layer facilitating charge transport.[36,39] The ternary blend film combines comprehensively the above advantages, obtaining the optimized surface morphology to increase the device performance.

### 3 Conclusions

In summary, we fabricated efficient ternary all-PSCs of using two analogous donors (PBCIT and PTB7-Th) and a polymer acceptor NDP-V-C7. The binary PBCIT:NDP-V-C7 PSCs exhibited a high  $V_{oc}$  of 0.93 V due to the deep HOMO of chlorination. The champion ternary device with an optimal ratio for two analogous donors and one acceptor obtained a high PCE of 9.03%. The PBCIT as extra donor was added into initial PTB7-Th:NDP-V-C7 all-PSCs system, the formed cascade energy levels were benefit to charge transfer for electrons and holes in resulted ternary all-PSCs. The ternary all-PSCs presented the more balanced electron and hole transport and prolonged carriers lifetime compared to the binary devices. The introduction of PBCIT in ternary blend could also enhance miscibility and suppress crystallization in films, resulting that ternary devices had favorable charge dynamics and morphology in blend film. Our study evidenced the ternary blend, especially using the analogue co-donors, was an effective strategy to enhance the all-PSCs performance and expanded the application of chlorinated photovoltaic materials in polymer solar cell field.

**Acknowledgments** The authors acknowledge financial support from SUSTech, the Recruitment Program of Global Youth Experts of China, the

National Natural Science Foundation of China (51773087, 21733005), the Natural Science Foundation of Guangdong Province (2016A030313637), Shenzhen Fundamental Research program (JCYJ20170817111214740) and Shenzhen Nobel Prize Scientists Laboratory Project (C17783101). W.C. gratefully acknowledges financial support from the US Department of Energy, Office of Science, Materials Science and Engineering Division.

**Conflict of interest** The authors declare that they have no conflict of interest.

**Supporting information** The supporting information is available online at <http://chem.scichina.com> and <http://link.springer.com/journal/11426>. The supporting materials are published as submitted, without typesetting or editing. The responsibility for scientific accuracy and content remains entirely with the authors.

- 1 Marrocchi A, Facchetti A, Lanari D, Petrucci C, Vaccaro L. *Energy Environ Sci*, 2016, 9: 763-786
- 2 Hou J, Inganäs O, Friend RH, Gao F. *Nat Mater*, 2018, 17: 119-128
- 3 He Z, Xiao B, Liu F, Wu H, Yang Y, Xiao S, Wang C, Russell TP, Cao Y. *Nat Photonics*, 2015, 9: 174-179
- 4 Lin Y, Zhan X. *Acc Chem Res*, 2016, 49: 175-183
- 5 Li Y. *Acc Chem Res*, 2012, 45: 723-733
- 6 Liu Y, Zhao J, Li Z, Mu C, Ma W, Hu H, Jiang K, Lin H, Ade H, Yan H. *Nat Commun*, 2014, 5: 5293
- 7 Zhang Q, Kan B, Liu F, Long G, Wan X, Chen X, Zuo Y, Ni W, Zhang H, Li M, Hu Z, Huang F, Cao Y, Liang Z, Zhang M, Russell TP, Chen Y. *Nat Photonics*, 2014: 9, 35-41
- 8 Kan B, Li M, Zhang Q, Liu F, Wan X, Wang Y, Ni W, Long G, Yang X, Feng H, Zuo Y, Zhang M, Huang F, Cao Y, Russell TP, Chen Y. *J Am Chem Soc*, 2015, 137: 3886-3893
- 9 Li S, Ye L, Zhao W, Zhang S, Mukherjee S, Ade H, Hou J. *Adv Mater*, 2016, 28: 9423-9429
- 10 Sun K, Xiao Z, Lu S, Zajaczkowski W, Pisula W, Hanssen E, White JM, Williamson RM, Subbiah J, Ouyang J, Holmes AB, Wong WW, Jones DJ. *Nat Commun*, 2015, 6: 6013
- 11 Fan Q, Su W, Wang Y, Guo B, Jiang Y, Guo X, Liu F, Russell TP, Zhang M, Li Y. *Sci China Chem*, 2018, 61: 531-537
- 12 Guo X, Zhou N, Lou S, Smith J, Tice DB, Hennek JW, Ortiz RP, Navarrete JTL, Li SY, Strzalka J, Chen LX, Chang RPH, Facchetti A, Marks TM. *Nat Photonics*, 2013, 7: 825-833
- 13 Liu J, Chen S, Qian D, Gautam B, Yang G, Zhao J, Bergqvist J, Zhang F, Ma W, Ade H, Inganäs O, Gundogdu K, Gao F, Yan H. *Nat Energy*, 2016, 1: 16089
- 14 Zhao W, Li S, Yao H, Zhang S, Zhang Y, Yang B, Hou J. *J Am Chem Soc*, 2017, 139: 7148-7151
- 15 Zhao J, Li Y, Yang G, Jiang K, Lin H, Ade H, Ma W, Yan H. *Nat Energy*, 2016, 1: 15027
- 16 Kan B, Feng H, Yao H, Chang M, Wan X, Li C, Hou J, Chen Y. *Sci China Chem*, 2018, 61, <https://doi.org/10.1007/s11426-018-9334-9>
- 17 Zhang S, Qin Y, Zhu J, Hou J. *Adv Mater*, 2018, 30: 1800868
- 18 Xiao Z, Jia X, Ding L. *Sci Bull*, 2017, 62: 1562-1564
- 19 Che X, Li Y, Qu Y, Forrest SR. *Nat Energy*, 2018, 3: 422-427
- 20 Zhang H, Yao H, Zhu J, Zhang J, Li W, Yu R, Gao B, Zhang S, J Hou. *Adv Mater*, 2018, 30: 1800613
- 21 Li S, Ye L, Zhao W, Yan H, Yang B, Liu D, Li W, Ade H, Hou J. *J Am Chem Soc*, 2018, 140: 7159-7167
- 22 Kolhe NB, Lee H, Kuzuhara D, Yoshimoto N, Koganezawa, T, Jenekhe SA. *Chem Mater*, 2018, 30: 6540-6548
- 23 Chen S, An Y, Dutta GK, Kim Y, Zhang Z, Li Y, Yang C. *Adv Funct Mater*, 2017, 27: 1603564
- 24 Gao L, Zhang Z, Xue L, Min J, Zhang J, Wei Z, Li Y. *Adv Mater*, 2016, 28: 1884-1890
- 25 Kim T, Kim JH, Kang TE, Lee C, Kang H, Shin M, Wang C, Ma B, Jeong U, Kim TS, Kim BJ. *Nat Commun*, 2015, 6: 8547
- 26 Kim W, Choi J, Kim JH, Kim T, Lee C, Lee S, Kim M, Kim BJ, Kim TS. *Chem Mater*, 2018, 30: 2102-2111
- 27 Li Z, Xu X, Zhang W, Meng X, Ma W, Yartsev A, Inganäs O, Andersson MR, Janssen RAJ, Wang E. *J Am Chem Soc*, 2016, 138: 10935-

10944

- 28 Kim T, Choi J, Kim HJ, Lee W, Kim BJ. *Macromolecules*, 2017, 50: 6861-6871
- 29 Hwang YJ, Courtright BA, Ferreira AS, Tolbert SH, Jenekhe SA. *Adv Mater*, 2015, 27: 4578-4584
- 30 Kim T, Younts R, Lee W, Lee S, Gundogdu K, Kim BJ. *J Mater Chem A*, 2017, 5: 22170-22179
- 31 Fan B, Ying L, Zhu P, Pan F, Liu F, Chen J, Huang F, Cao Y. *Adv Mater*, 2017, 29: 1703906
- 32 Guo Y, Li Y, Awartani O, Han H, Zhao J, Ade H, Yan H, Zhao D. *Adv Mater*, 2017, 29: 1700309
- 33 Hwang YJ, Earmme T, Courtright BAE, Eberle FN, Jenekhe SA. *J Am Chem Soc*, 2015, 137:4424-4434
- 34 Lu L, Xu T, Chen W, Landry ES, Yu L. *Nat Photonics*, 2014, 8: 716-722
- 35 Hwang YJ, Courtright BA, Jenekhe SA. *MRS Commun*, 2015, 5: 229-234
- 36 Li Z, Ying L, Xie R, Zhu P, Li N, Zhong W, Huang F, Cao Y. *Nano Energy*, 2018, 51: 434-441
- 37 Liu T, Guo Y, Yi Y, Huo L, Xue X, Sun X, Fu H, Xiong W, Meng D, Wang Z, Liu F, Russell TP, Sun Y. *Adv Mater*, 2016, 28: 10008-10015
- 38 Gasparini N, Jiao X, Heumueller T, Baran D, Matt GJ, Fladischer S, Spiecker E, Ade H, Brabec CJ, Ameri T. *Nat Energy*, 2016, 1, 16118
- 39 Li Z, Xu X, Zhang W, Meng X, Genene Z, Ma W, Mammo W, Yartsev A, Andersson MR, Janssen RAJ, Wang E. *Energy Environ Sci*, 2017, 10: 2212-2221
- 40 Hu Z, Chen H, Zhong X, Qu J, Chen W, Liu A, He F. *Acta Polymerica Sinica*, 2018, 2: 273-283.
- 41 Chao P, Mu Z, Wang H, Mo D, Chen H, Meng H, Chen W, He F. *ACS Appl Energy Mater*, 2018, 1: 2365-2372
- 42 Chen H, Hu Z, Wang H, Liu L, Chao P, Qu J, Liu A, Chen W, He F. *Joule*, 2018, 2: 1623-1634
- 43 Wang Z, Zhang Y, Zhang J, Wei Z, Ma W. *Adv Energy Mater*, 2016, 6: 1502456.
- 44 You J, Meng L, Song TB, Guo TF, Yang YM, Chang WH, Hong Z, Chen H, Zhou H, Chen Q, Liu Y, Marco ND, Yang Y. *Nat Nanotechnol*, 2016, 11: 75-82
- 45 Kyaw AKK, Wang DH, Luo C, Cao Y, Nguyen TQ, Bazan GC, Heeger AJ. *Adv Energy Mater*, 2014, 4: 1301469
- 46 PN Murgatroyd. *J Phys D: Appl Phys*, 1970, 3: 151-156
- 47 Shuttle CG, O'Regan B, Ballantyne AM, Durrant JR. *Appl Phys Lett*, 2008, 92: 093311
- 48 Cowan SR, Street RA, Cho S, Heeger AJ. *Phys Rev B*, 2011, 83: 035205
- 49 Hu Z, Chen H, Qu J, Zhong X, Chao P, Xie M, Lu W, Liu A, Tian L, Su Y, Chen W, He F. *ACS Energy Lett*, 2017, 2: 753-758

### Table of Contents graphic

